JACS
JOURNAL OF THE AMERICAN CHEMICAL SOCIETY
Article
pubs.acs.org/JACS

Studies of Aluminum Reinsertion into Borosilicate Zeolites with Intersecting Channels of 10- and 12-Ring Channel Systems

Stacey I. Zones,*[†] Annabelle Benin,[†] Son-Jong Hwang,[‡] Dan Xie,[†] Saleh Elomari,[†] and Ming-Feng Hsieh[†]

[†]Chevron Technology Company, Richmond, California 94802, United States
[‡]California Institute of Technology, Pasadena, California 91125, United States

Supporting Information

ABSTRACT: The work here describes the kinetic analyses of aluminum replacement for boron in a suite of borosilicate molecular sieves. While the method has been described before as a means of converting synthesized borosilicates (with weak inherent acidity) to aluminosilicates (with much stronger acid strength) when there are large pores in the structure, here we carry out the transformation under less than optimal replacement concentrations, in order to better follow the kinetics. We examined several zeolite structures with boundary conditions of boron MEL where there are only 10-ring (or intermediate) pore structures and no Al is taken up, to multidimensional large pore zeolites, like boron beta, where Al substitution can occur everywhere. We also studied materials with both intermediate and large pores, SSZ-56, 57, 70, and 82. In the case of 57 up to 90% of the structure is made up of boron MEL. We observe that the pH drop is proportional to the Al reinsertion and is the same for all zeolites we studied. In one case, we compared a zeolite (SSZ-24) with boron and then no boron sites and found that Al does not go into defect sites. It was again confirmed (shown in earlier work) that Al will go into nest sites created by boron hydrolysis out of the substrate before Al treatment. Along those lines we also made two new observations: (1) the profile for Al uptake, as followed by pH drop, is the same kinetically, whether the boron is there or not; and (2) NMR showed that the boron is leaving the structure faster than Al can go back in (SSZ-33 study), even when we treat a material with boron in the lattice.

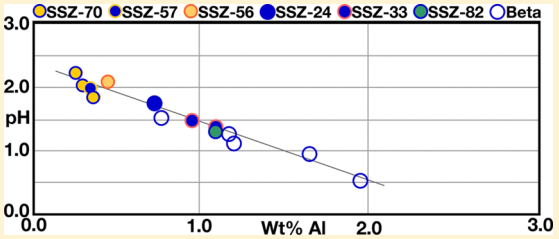

INTRODUCTION

Zeolitic materials with micropores ranging from roughly 4 to 12 Å have blossomed into materials of great technological value over the past half-century. As synthetic porous crystalline solids they have found utility in catalysis for fuels and petrochemicals and as adsorbants for separations in a variety of chemical-based process technologies.[1] Synthesis efforts continue to find new crystalline structures[2] as the inorganic and organic chemistry is varied. While only a minority of discoveries advance to the commercial development stage,[3] there is still value in empirical trials to elucidate successful materials to develop.[4] Also, in the background, there is the steady advance of approaches where one can computationally design a zeolite, optimized for a process.[5,6]

With regard to application, improvements in performance can result from further additional modifications of a given structure. Changes in chemical composition,[7] crystalline size,[8] or in homogeneity in the pore systems, allow for better diffusion to and from active sites in so-called hierarchical zeolite,[9−12] have all produced desirable advances. While earlier focus on zeolites as catalysts often focused on shape selectivity imparted from the pore sizes of various materials,[13−17] it may be easier to compare the bigger factor of pore sizes and reactant (or product exit) selectivity that is increasingly emerging through transition-state selectivity. Most uses of zeolite materials as catalysts focus on the contribution of strong solid acid sites within the pores. Some evaluation of catalytic performance has concentrated on internal space created by virtue of the crystalline architecture.[18−22] More recently focus has moved to the possibility that specific parts of a given zeolite structure might support catalytic specificity. A key example has been the discovery by the group of Iglesia that 8-ring site pockets, off of a large 12-ring channel, can be preferred locations for small molecule transformation.[23−25] Figure 1 shows a representation of such a site pocket in zeolite mordenite. Guisnet et al.[26] have done studies in how the various spatial regions in zeolite **MWW** can contribute to overall reaction selectivity. Even more recently work has focused on coupling computational approaches to develop a further understanding of the zeolite host lattice as contributing a solvation parameter (mostly van der Waal's in nature) to support transition states along a reaction coordinate.[27−30]

We recently encountered a novel zeolitic structure that contained domains of unusual internal features. This differed from all other known zeolites in that the new structure contains segments where there is no interface with other segments (in most zeolites built of more than one type, the types typically intersect with each other in a given unit cell of the material). This novel material, SSZ-57 (***SFV**),[31−34] is dominated by

Received: October 7, 2013
Published: January 8, 2014

   dx.doi.org/10.1021/ja4100194 | J. Am. Chem. Soc. 2014, 136, 1462−1471

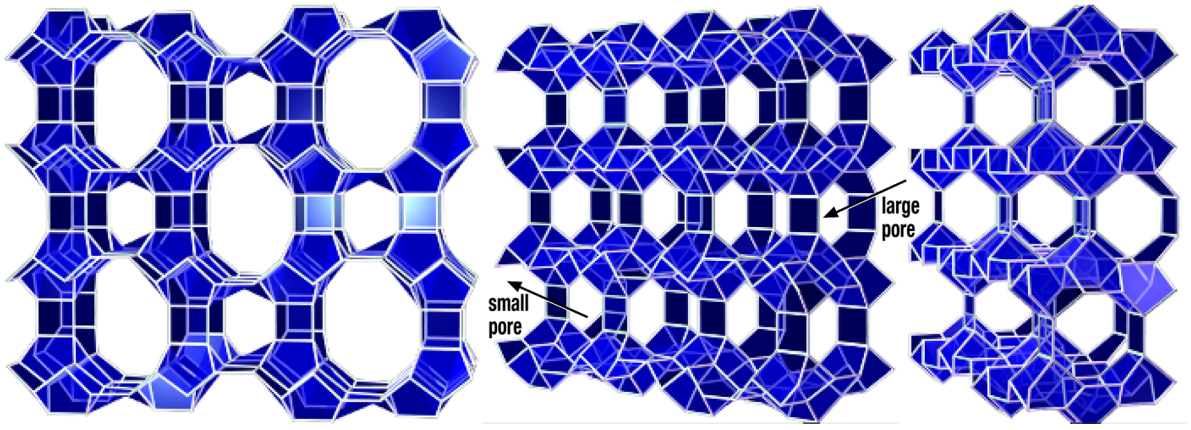

Figure 1. MOR, shown in three-step rotation.

intersecting pores of 10-rings (termed intermediate pores) but interrupted every 110 Å by isolated, distorted single lengths of a large pore. An art rendering is given in Figure 2. When SSZ-57

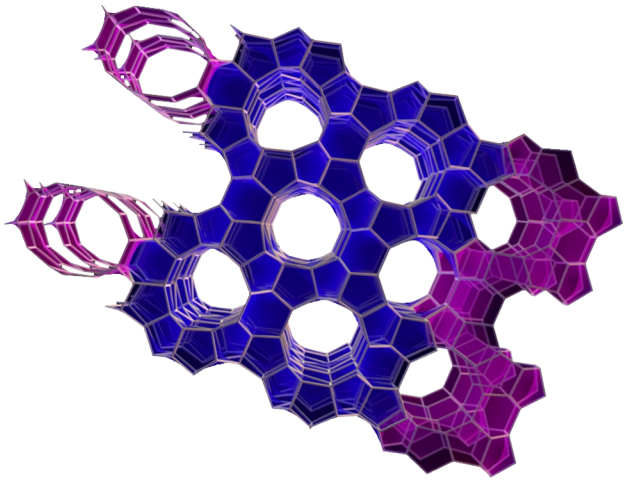

Figure 2. SSZ-57.

is made with Al as a substituent there are catalytically active sites in both domains of the structure, and the result is a lumped contribution in examining the performance of the catalyst. These results were seen when the structure of the novel zeolite was not yet understood.[32,35] But the zeolite can also be made with B as a lattice substituent, and this material contains sites too weak in acid strength to carry out many hydrocarbon conversions. Using this fact, and coupling it with our knowledge that one can replace B with aluminum in frameworks under acidic conditions,[36,37] but only if the pores are large,[38] allowed us to create a new catalytic material, SSZ-57LP, where the strong acid sites are only in the large pores periodically found in the zeolite structure. Indeed, the reaction of such a material generated changes in catalytic selectivity over SSZ-57 with Al sites throughout the structure.[38,39]

In this contribution we study, in some detail, the aluminum reinsertion reaction as carried out on B SSZ-57. To better understand some of the effects of time and reactant concentration, we include several other borosilicate zeolites in the study. While a goal of the study was a kinetic description of the substitution reaction, what has emerged is the prospect that the reaction itself may provide an indication of 10- and 12-ring intersection in novel borosilicate zeolites whose structure may not have yet been determined.

EXPERIMENTAL SECTION

Preparation of Zeolite Materials. The zeolites used in the study have a synthesis reference given in Tables 1a and 1b. In order to be used in the experiments, these borosilicates were calcined in thin beds with nitrogen flowing over the solids (20 cu ft/min) with about a 2% mix of air introduced. The calcination program was 23−120 °C at 1°C/min, hold at 120 °C for 2 h, then to 550 °C at 1 °C/min and hold at 550 °C for 5 h, then cool to 30 °C. Micropore volumes are also given in Table 1a for nitrogen.

Table 1a. Zeolites in This Study

zeolite	wt % B	wt % Si	Si/B	micropore volume[a]	synthesis ref
B SSZ-57	0.38	41	42	0.17	39
B SSZ-33	0.61	40	26	0.20	40
B SSZ-70	0.51	42	32	0.20	41
B SSZ-56	0.61	40	26	0.18	42
B SSZ-82	0.87	39	18	0.18	43
B beta	1.10	30	11	0.25	44
B SSZ-24	0.45	42	35	0.12	45
B UCB-4	0.50	42	32	0.16	46
B MEL	0.50	42	32	0.15	47

[a] cc/g.

Table 1b. Codes and Channel Dimensions for Zeolites in This Study

B SSZ-33	**CON**	12−12−10
B SSZ-70	none	?
B SSZ-56	**SFS**	12−10
B SSZ-82	**SEW**	12−10
B SSZ-57	***SFV**	10−10, 12
B beta	**BEA**	12−12−12
B SSZ-24	**AFI**	12
B UCB-4	none	?
B MEL	**MEL**	10−10

Method of Aluminum Reinsertion into Borosilicates. A typical run[39] was to use 0.40 g of calcined borosilicate, 0.10 g of $Al(NO_3)_3 \cdot 9H_2O$, and 10 mL H_2O. The solution with aluminum nitrate in 10 mL of water, when measured at room temperature and before adding the zeolite, has a pH of 3.5. The vial with all three components was heated to 95 °C, static and time points (individual vials) were removed at specified times, was cooled, and had solution and solids separated. The solids were typically washed twice with pH = 2 HCL

dx.doi.org/10.1021/ja4100194 | J. Am. Chem. Soc. 2014, 136, 1462−1471

solution, at room temperature, to remove any solubilized Al salt before continuing to water wash. In some experiments, where specified, reactant ratios were changed.

Deboronation. In one series, the boron was removed before the study of the rates of Al reinsertion. The pretreatment consisted of heating (95 °C) the zeolite in pH = 2, HNO_3 solution. Heating was carried out for 3 days, and then solids were collected, washed, and dried at 95 °C before use.

The pH measurements were made as follows: A Thermo Scientific meter equipped with an Orion 8157BNUMD Ross Ultra Triode was used to make pH measurements. Electrode calibrations were performed using the following buffer solutions: pH = 4.01 (Thermo Scientific, pink), pH = 7.00 (Fisher, yellow), pH = 10.00 (Fisher, blue), and electrode was stored in a pH electrode storage solution (Thermo Scientific). All measurements were collected at room temperature. Prior to each set of experimental pH measurements, a two-point calibration was performed in the range of interest. pH measurements were also made on standards for pH solutions = 1, 2, and 3. For these solutions the electrode we used, calibrated on the other buffered standards, had an error of +0.05 to 0.10 for each pH solution at 1, 2, or 3. It is expected that there will be a greater degree of electrode error at the very low and very high pH media.

Elemental Analyses. After the exchange treatment, solids were sent to Galbraith Laboratories for determination (ICP method) of weight % Al added, B remaining, and Si.

NMR Measurement of Solids. ^{11}B or ^{27}Al MAS NMR spectra of zeolite samples were recorded after a short single pulse (nutation angles of $\pi/12$ and $\pi/18$ for ^{11}B and ^{27}Al, respectively) and with strong ^{1}H decoupling using a DSX-500 spectrometer and a Bruker 4 mm CPMAS probe. Samples were spun typically at 14 kHz at room temperature after the powders were packed into zirconia rotors at ambient conditions. Spectra were reported in part per million after calibration with external reference of $BF_3 \times O(CH_2CH_3)_2$ for ^{11}B nucleus and 1 M $Al(NO_3)_3$ aqueous solution for ^{27}Al nucleus. ^{11}B solution NMR spectra were recorded for 100 μL of solutions that were loaded into a 4 mm zirconia rotor and using a $\pi/2$ pulse and ^{1}H decoupling.

RESULTS

In our previous work[39] we demonstrated that for zeolite SSZ-57 the large pores could have Al replace B, but not in the intermediate pores. We showed comparative data for pH drop for SSZ-57, ZSM-11 (where none is expected), and SSZ-33 (where Al can likely go everywhere).[36−38] Picking up this theme, Figure 3 shows the pH drop with time for SSZ-57. Table 2 shows the starting B content and then pH drop and replacement by Al with time of treatment at 95 °C. We can understand the behavior of Al replacement for B in SSZ-57 by two of our experiments. In Table 3 one sees the results of changing the initial Al concentration in the reaction for Al for B in a final SSZ-57. Even with changes in starting Al content the final values stayed fairly constant, indicative of possibly reaching a maximum in the substitution of Al for B in SSZ-57. The replacement would be about 10% of the sites for a SSZ-57, synthesized directly with Al, where the lattice substitution can be throughout the structure. 10% replacement would be consistent with the relative void space contribution for the large pore portion of the SSZ-57 structure (Figure 2). On the other hand, we can also ask what happens when we vary the B content (by synthesizing B SSZ-57 with different B reagent content) and conduct the Al replacement solution. The pH data and elemental analyses are in Table 4. Here, there is some variation in the final pH value and the amounts that Al is taken up. This would be consistent with the overall B content in the large pores being higher as a result of differing B in the initial zeolite.

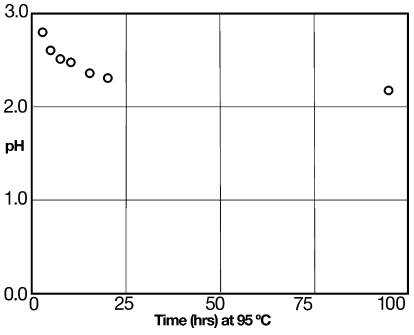

Figure 3. Changes in pH for SSZ-57 solutions versus time of treatment at 95 °C.

Table 2. Al Reinsertion into B SSZ-57 with Time[a]

time (h)	pH	wt % Al
3	3.02	0.14
6	2.85	0.12
9	2.76	0.14
30	2.39	0.23
96	2.24	0.29

[a]95 °C, static, see text for reactant ratios.

Table 3. Effect of Varying the Aluminum Nitrate Reagent Concentration for Treatment of B SSZ-57

mass $Al(NO_3)_3$	final pH	wt % Al
3.75	2.29	0.245
1.80	2.06	0.300
0.45	2.00	0.330
0.22	2.03	0.330
0.045	2.22	0.300

Table 4. Al Reinsertion Back into B SSZ-57 When the Boron Content Has Varied in the Latter

initial wt % B	pH 20 min	pH 96 h	wt % Al
0.384	3.35	1.99	0.384
0.335	3.54	2.15	0.346
0.288	3.76	2.30	0.298
0.255	3.79	2.37	0.269
0.195	3.97	2.63	0.240

As had been pointed out by Chen[38] one can remove the B from a large pore zeolite like SSZ-33 in a single step with acid hydrolysis and then follow-up in a second step with Al $(NO_3)_3$ solution and get reinsertion of Al into the vacancy left by the departing B. Figure 4 shows an interesting comparison of the pH drop as Al goes into SSZ-57, whether the B is still in the zeolite or already hydrolyzed out. The data show that rates (based upon pH drop) are almost identical. We will have more to discuss about the aluminum reinsertion mechanism below.

To better understand the behavior for B SSZ-57 we can contrast B MEL where there are only intermediate pores in the multidimensional zeolite structure (and remember this is the main structural domain of SSZ-57) and a multidimensional large pore zeolite like B SSZ-33, where Al should be able to go everywhere in the structure. Chen had already shown that the Al replacement can be complete if the reagent content is great enough (Table 5). Under two same reagent run conditions,

dx.doi.org/10.1021/ja4100194 | J. Am. Chem. Soc. 2014, 136, 1462−1471

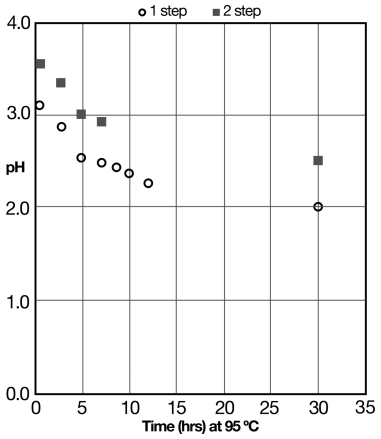

Figure 4. Direct Al insertion into B SSZ-57 and then Al into deboronated SSZ-57 (two-step).

Table 5. Effect of Increasing the Aluminum Nitrate Reagent on the Final Si/Al Zeolite Product Values after B SSZ-33 Being Treated[a]

mass of SSZ-33 (g)	Si/B	$Al(NO_3)_3 \cdot 9H_2O$ (g)	H_2O	product Si/Al
–	18	–	–	–
1	–	6.4	13	25
1	–	10	20	20
1	–	20	40	17

[a]4 days at 100 °C; after ref 38.

Figure 5 picks up the pH drop for the use of **CON** and **MEL** versus time in the experiment. There is almost no drop at all for

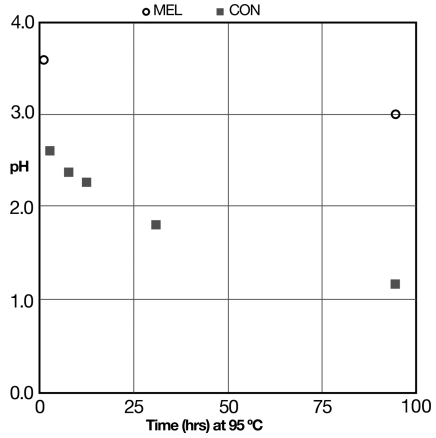

Figure 5. pH drop for Al reinsertion into SSZ-33 (**CON**) and ZSM-11 (**MEL**).

MEL and considerable for SSZ-33. Table 6 contrasts the Al substitution for these three materials, which represents the three cases.

Other Zeolites with Both Large and Intermediate Pores. Next we explored some zeolites with mixed pore systems. Recently the delaminating of SSZ-70 to UCB-3 (this latter material is the delaminated product form using Al-SSZ-70 where the Al is in the initial synthesis) was described.[48] A comment was made in that work that a delaminated B version of SSZ-70 (termed UCB-4 for the delaminated material) could be repopulated, to a certain extent, by using the Al reinsertion approach described here. Subsequent studies indicated that the

Table 6. pH Change with Time For Al Reinsertion Into B SSZ-33 versus B MEL[a]

zeolite	final pH at 96 h, 95 °C	wt % Al after 96 h, 95 °C
ZSM-11 (**MEL**)	3.00	0.01
SSZ-57 (**SVR**)	2.24	0.30
SSZ-33 (**CON**)	1.36	1.10

[a]See text for reagent values.

catalytic performance of the Al-UCB-4 (where Al has been put back into the delaminated borosilicate precursor, UCB-4, as will be discussed here) was consistent with large pore character.[49] And yet, we knew that we do not get full replacement of B by Al. A more detailed analysis here also gives that picture. Figure 6 shows the pH drop for Al substituting into B SSZ-70 with

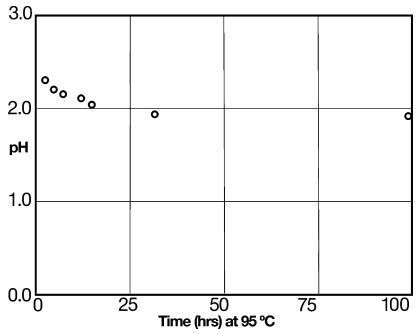

Figure 6. pH drop for Al reinsertion into SSZ-70.

time. The profile is similar to SSZ-57 bottoming out at final pH near 2. Table 7 shows the Al contents for the various time

Table 7. Reinsertion of Al into B SSZ-70 as a time study[a]

time (h)	pH	wt % Al
2	2.28	0.07
4	2.18	0.08
6	2.14	0.11
8	2.12	0.13
10	2.13	0.14
12	2.04	0.15
24	2.00	0.19
60	1.83	0.19
96	1.90	0.28

[a]See text for reagent values.

points. Compared with a material like SSZ-33, the Al replacement is far less. Table 8 shows a set of experiments

Table 8. Al Reinsertion[a] **into B SSZ-70 When Boron Content Is Variable**

boron content	final pH (96 h, 95 °C)	wt % Al
0.360	1.85	0.400
0.305	1.91	0.365
0.280	2.01	0.321
0.230	2.14	0.302
0.220	2.12	0.227

[a]Conditions for treatment were 0.15 gms B SSZ-70, 0.569 g of $Al(NO_3)_3 \cdot 9\ H_2O$, 3.8 g of water heated, and the samples were heated at 95 °C for 5 days. The workup is the same as described in the Experimental Section.

dx.doi.org/10.1021/ja4100194 | J. Am. Chem. Soc. 2014, 136, 1462−1471

where, via synthesis of variable B SSZ-70,[49] one can see variation in the final pH value and therefore the Al^{3+} substitution, as a result of starting with variable B in SSZ-70 and holding all other reactant ratios constant. While the higher initial B value leads to a higher final Al content in product, the values fall far short of what is observed for SSZ-33.

While the structure of SSZ-70 is still not known, our data hint at it having some 12 rings, and there are four other zeolites with both 12- and 10-ring portals. We will describe studies on SSZ-56 and SSZ-82 where there are two of these four 10−12 intersecting systems. Also, it has other features that are not accessible to Al (see, for example, the micropore volume in Table 1a). It has been mentioned in the past that a number of newly discovered zeolites are only accessible, synthetically, as the borosilicate product.[50] The hope is that if there are large pores, then Al can substitute for B in the structure. Zeolites SSZ-56 and SSZ-82 are two such structures that require the initial synthesis to use B, but the final product can have the 12-ring sites replaced with Al.[42,43] Representation of their channel structure, along with the other zeolites in this study, is given in Appendix I as part of Supporting Information. The pH and Al content changes for SSZ-56 and SSZ-82 are summarized in Table 9 as well as with data for the other zeolites mentioned

Table 9. Al Reinsertion pH Changes for Several B Zeolites under Same Mass Ratios

	final pH					
time (h)	SSZ-57	SSZ-70	SSZ-33[a]	SSZ-56	UCB-4	SSZ-82
2	3.01	2.28	2.47	2.45	1.95	1.60
4	2.87	2.18	2.29	2.28	1.75	1.49
6	2.71	2.14	2.18	2.19	1.70	1.49
8	2.78	2.12	–	2.13	1.65	1.45
30	2.51	1.90	1.83	2.02	1.60	1.35
96	2.24	1.90	1.36	2.08	1.66	1.34

[a]Results for the two-step experiment after boron removal.

(including treatment of the delaminated B SSZ-70 = UCB-4). Interestingly, the two known 12−10 intersecting pore structures diverge in their response with B SSZ-56 showing a limit of replacement (like SSZ-57 and 70). SSZ-82 behaves as though Al can replace B throughout the structure.

The High End of Al Replacement. Looking at the initial B values in Table 1a and comparing the Al contents of the products, it is clear that our run conditions do not give a complete substitution of B for Al when it is possible, as in SSZ-33. Consulting Table 5, where some of Chen's data[38] are reproduced, it can be seen that the use of a sizable excess of Al^{3+} cation in acidic solution conditions can replace all of the B. While we did not want to go to the excess of reagent desired by Chen, we were interested in what happened to the pH drop as the Al content in the final product went beyond 1 wt %. Instead of doing further work with SSZ-33, we used B beta zeolite, a three-dimensional set of large pores where Al should be able to go everywhere. Also, the B beta has a higher initial B content of 1.1 wt %. In theory, this could lead to an Al product with 2.7 wt %.

Table 10 shows our choices of Al reagent content for these experiments and then the final pH and Al contents. A plot of Al product content versus final pH value shows a nice linear fit, and this will help us develop more understanding of the Al reinsertion chemistry. Figure 7 shows this correlation.

Table 10. Variable $Al(NO_3)_3 \cdot 9H_2O$ Reagent Treatment for B beta (1.1 wt % B) 0.40 g Z + 10 mL H_2O[a]

mass $Al(NO_3)_3 \cdot 9H_2O$ (g)	Al/B ratio	final pH (96 h)
0.000	0.00	5.65
0.100	0.20	1.54
0.375	0.70	1.26
1.000	2.00	1.12
2.000	4.00	0.95
5.000	10.00	0.56

[a]Addition of Al reagent adds increasingly more H_2O, so all runs were adjusted to same H_2O mass.

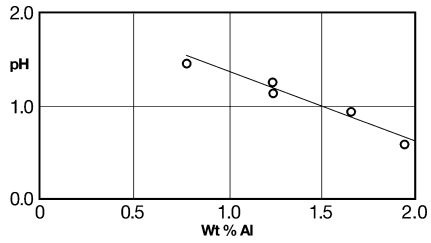

Figure 7. pH drop versus Al uptake in B beta.

Al Reinsertion and Defect Sites. A good correlation for Al going into vacant silanol nests had been emerging. Still, we had not answered the question of whether a nest of Si−OH was needed or whether a single Si−OH could anchor any Al. Part of the answer came in our previous study where we replaced only a fraction of B with Al (in creating SSZ-57LP) in the B SSZ-57 system. An analysis of the Al in the product, after the reinsertion and before any calcination, showed that almost all of the Al was tetrahedral, as seen by MASNMR.[39] A very small amount of octahedral Al can be seen.

The following experiment seemed to be a more direct view about the possibilities of the Al anchoring into a single Si−OH defect site. In using large pore one-dimensional zeolite SSZ-24 (**AFI** structure and seen in Appendix I) the borosilicate and all-silica versions could be synthesized. In the borosilicate the Al is expected to be able to access all sites. The all-silica material might be expected to have a single anionic charge, Si−O−, in the wall to counterbalance the $Me3N^+$-adamantyl cation. In fact studies by Koller et al. showed that the site is likely an anion stabilized by other Si−OH as a nest as we have been discussing in this work.[51] Upon calcination this could become a Si−OH site. Table 11 shows the pH profiles for the time study of the two materials. It can be seen that SSZ-24 with B shows a pH drop and a final Al content of near 0.7 wt %. The all-silica material shows a pH value similar to B ZSM-11 as though no Al substitution had taken place. The Al analysis actually shows

Table 11. Time Study for Al Reinsertion Back into SSZ-24 (AFI structure) with and without Boron in the Zeolite

time (h)	pH for B SSZ-24	pH for SiO_2 SSZ-24
0.33	3.40	4.05
2	2.30	3.66
4	2.20	3.66
6	2.16	3.66
8	2.09	3.59
32	1.87	3.23
96	1.74[a]	3.03[b]

[a]0.72 wt % Al in product. [b]0.15 wt % Al in product.

dx.doi.org/10.1021/ja4100194 | J. Am. Chem. Soc. 2014, 136, 1462−1471

some Al in the product at a low level, and it is not clear if this is an attachment of Al precipitate or within the error of the measurement. A concern was whether the hydrated Al cation might have trouble entering the pores of the hydrophic zeolite material. So borrowing on the experiences of Davis et al. with hydrophobic zeolites[52] and the studies of Koller on B beta,[53] we repeated the Al treatment using ethanol as solvent. While a pH trend might not be seen, we could still get the Al reinsertion values, and the treatment with aluminum nitrate dissolved in 100% ethanol showed no Al uptake into the zeolite.

DISCUSSION

Boron in the Initial Zeolite. In these experiments we have started with calcined borosilicate samples where the B is in the zeolite. There is good indication that B is in a tetrahedral environment in the as-made zeolite. But there is already considerable change upon calcination. Both Hwang[54] and Koller[53] have shown these changes for borosilicates like SSZ-33 and beta in their respective studies. Figure 8 shows these

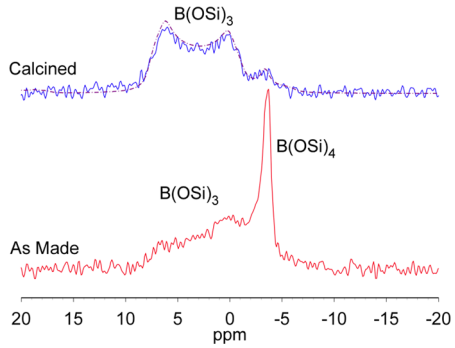

Figure 8. MASNMR spectra for boron in SSZ-57. As-made showing mostly tetrahedral location for B, and calcined material where most B is now trigonal. The ^{11}B spectral trace of the calcined sample is simulated (dashed line) using ^{11}B quadrupole NMR parameters reported for a trigonal unit, B[3]$_3$, of B beta.[55] ^{11}B NMR showed that after calcination, boron is found over 97% in the trigonally coordinated unit, B[3], while the as-made B-SSZ-57 contains higher B[4] units (~65%).

changes for B SSZ-57, one of the materials under study here. Using the assignments from both Hwang and Koller, upon calcination much of the B reverts to trigonal states and is easily hydrolyzed in subsequent exposure to water. An attempt was made to describe the decrease in connectivity to the lattice in these stages of hydrolysis as followed by NMR.[53,54] In our present study we can see (Table 10) that the treatment of B beta with only water and no Al$(NO_3)_3$, with an ending pH of near 5.6, still shows an almost complete loss of B. Further, we saw in our time study for Al replacement into B SSZ-33 that an NMR analysis of the solution samples during the treatment showed a rapid increase and leveling for B in solution within hours (see Figure 9). As we demonstrated once again, we obtain almost the same profile for Al uptake regardless of whether the B is present at the start of the experiment.

The Solution/Solid Equilibrium for Al Going into the Zeolite. One of the interesting findings in the replacement of B by Al in beta, as a function of initial Al$(NO_3)_3$ concentration in solution, was a near linear relationship for protons measured (pH) versus the Al placed into the lattice. This relationship would not hold if there was much of a hydrolysis product for the hydrated Al cation, as a function of concentration in solution. Indeed, fundamental studies of the hydrated cation demonstrate that this effect is small[55] and should not have much impact on the measured pH.

We can extend the data in Figure 7 by adding the other experiments for pH versus Al content onto the beta zeolite data. We see, remarkably, that our other results also fit this line (Figure 10). This tells us that the event observed, Al insertion and release of protons, is independent of zeolite structure.

If we run our reactions in 10 mL of water and then measure pH at room temperature, we are measuring millimoles of protons (e.g., pH = 2 is 10 millimoles H^+). But the unit of measurement is defined as per liter. So, if we normalize events to amount of borosilicate zeolite we start with, measure the wt % Al reinserted back in, we then find a roughly 3:1 ratio for protons in solution and millimoles of Al in product. Scheme 1 gives a depiction of such an exchange for hydrated aluminum cations becoming transposed to lattice substituents in tetrahedral configurations. We had shown in a previous study that the initial product, after the Al^{3+} treatment washing out in HCl aqueous solution (pH = 2), yields material with >90% Al cations in a tetrahedral configuration as measured by ^{27}Al MASNMR for SSZ-57 LP.[39] The same behavior is seen after the material is calcined. Hence, we think Scheme 1 is a reasonable representation of the reinsertion, producing strong acid sites as well. The consistent behavior, in the pH versus wt % Al plot (Figure 10) for several different zeolites, suggests that the behavior in a given B site is the same. The type of Al attachment is not changing with the different zeolite host architectural changes. The reinsertion produces strong acid sites, as was shown in a detailed study of zeolite SSZ-33 when the sites were created by exhaustive replacement of B by Al. The combined FTIR and MASNMR study demonstrated that SSZ-33 has strong acid sites, though the FTIR data suggest there may be some perturbation of the Bronsted site, perhaps being an asymmetry in the Al tetrahera.[56]

We then find a roughly 3:1 ratio for protons in solution and millimoles of Al in product for zeolites like SSZ-33, which exchange quite a bit of Al for B. We were initially excited that this relationship would hold over the range we studied. The data actually show that at higher pH the relationship begins to look more like a 2:1 relationship, and then at the very low values for a few of the beta zeolite exchanges, the ratio extends in the opposite direction. It is sensible that if we have a linear fit for a log/linear relationship of two variables, we will not have a linear correlation (3:1) over a long range. We do not believe that errors at low pH are sufficient to account for the deviations from this ratio observed. Nonetheless, the steady drop of pH with Al uptake provides a good indicator of how well Al is replacing boron sites. The overall reaction is represented in Scheme 1.

The 12−10 Intersecting Pore Systems. One of the exciting aspects of the study is to observe differential pH profiles when the Al cations appear to be hindered in accessing all parts of the zeolite structure. So, the initial boundary conditions were that **MEL** (10 × 10 multidimensional pore system) appeared to take up no Al as replacement for B. The 12 × 12 × 10 ring system of SSZ-33 appears to see no limit for exchange. This was likewise confirmed for beta zeolite. The value in studying B MEL, and seeing no uptake, provided better understanding of SSZ-57. The majority of its structure is **MEL** domains, but there was still a minor exchange of Al for B, confirming aspects of the model proposed by McCusker, Baerlocher, and colleagues.[34] Further, confirmation came from

dx.doi.org/10.1021/ja4100194 | J. Am. Chem. Soc. 2014, 136, 1462−1471

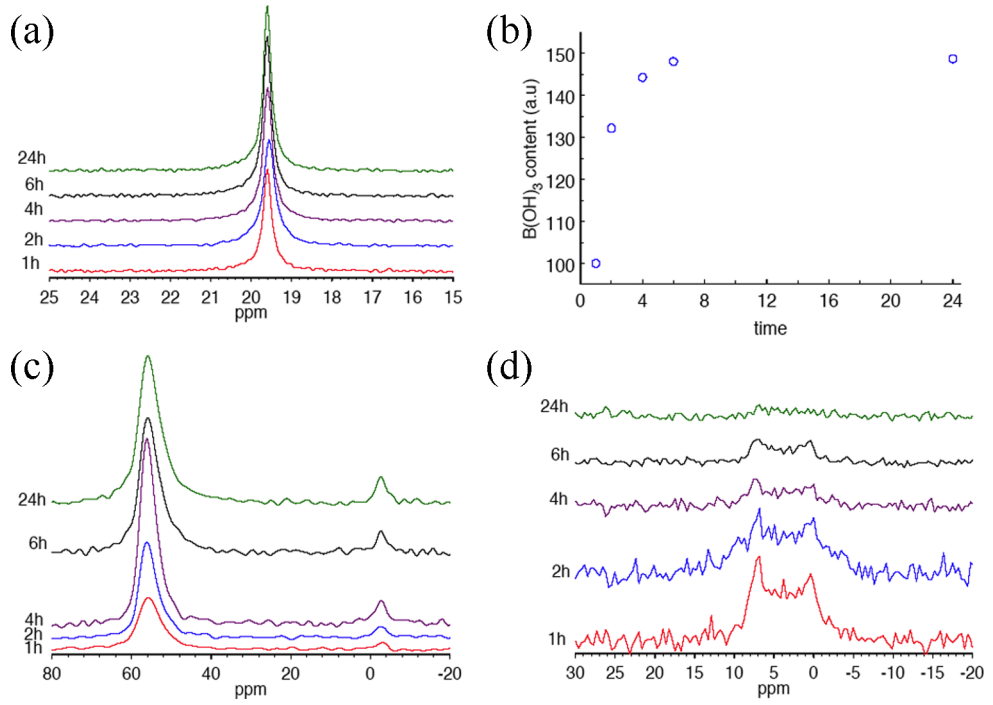

Figure 9. Changes in the state of Al and B (in solids and solution) for SZZ-33 during reinsertion of Al for B as a function of time. (a) Growth of boric acid in solution with time for B peak growing in. (b) Same data but as a concentration versus time. (c) The increase in tetrahedral Al in the SSZ-33 framework, and (d) the loss of the boron signal in the solid SSZ-33 with time.

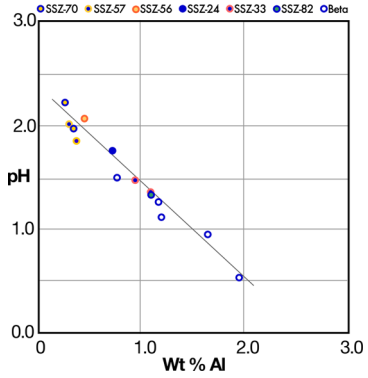

Figure 10. pH versus Al uptake in product.

Scheme 1. Replacement of Boron in Zeolite Lattice by Al^{+3} Cations

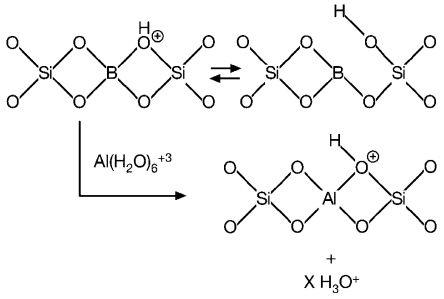

the changes in catalysis for the Al into SSZ-57 (SSZ-57 LP) as compared to Al-synthesized SSZ-57. Zones, Chen, and colleagues recently described these changes.[39]

More than a decade ago, Corma et al. had indicated the changes in diffusion and reaction selectivity such 12−10 intersecting channels might possess.[57] Since that time, materials with 12- and 10-ring channels that intersect have been created synthetically. In this study we examine zeolites SSZ-56 and SSZ-82 as transformed from borosilicates to aluminosilicates. The synthetic boggsite (**BOG**, ITQ-47)[58] fits well in this group, but was not studied here. In discussing our observation on zeolites SSZ-56 and -82, an important contrast is that zeolite SSZ-57 also has 12−10 intersection regions, but additionally many more sites where the intersections are only 10−10. SSZ-57 stands alone in having these noninteracting special domains.

In replacing B with Al in SSZ-57, there seems to be an upper limit of near 0.40 wt % Al achieved, regardless of some variation in either initial B content (Table 3) or the excess of Al reagent used (Table 4). In turn, the pH drop hovers near 2 and is consistent with the protons generated in relation to Al uptake, as shown in Figure 10. The two values measured give a picture of a minor replacement of B by Al in a material with good micropore volume (Table 1a). Now if we move to SSZ-56 and -82, both systems with intersecting 10- and 12-ring channels, we observe a differential response to the treatment experiment. While SSZ-56 loads more Al than SSZ-57, the pH drop is in the same region (Table 9). This would imply that Al will not access all parts of SSZ-56. In contrast, SSZ-82 shows a much greater uptake of Al and generation of protons. In this regard, SSZ-82 is seen to behave much more like SSZ-33 (**CON**), a 12−12−10 system.

A matter to examine, then, is the issue of where the B might be sited in either SSZ-56 or -82. If the B is always at an intersection, then it may be possible to replace all of it with Al. In Figure 11 key segments of the two zeolites are reproduced.[42,43] One of the key considerations is the population of B in 4-rings within the structures. In a past study on how a single SDA would make either large pore multidimensional frameworks like B SSZ-33 or higher framework density one-dimensional systems like B SSZ-31, we

dx.doi.org/10.1021/ja4100194 | J. Am. Chem. Soc. 2014, 136, 1462−1471

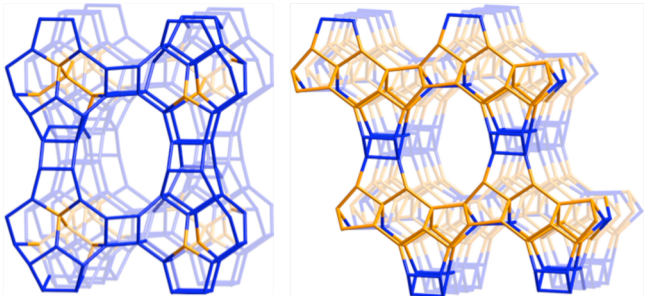

Figure 11. Comparison of SSZ-82, **SEW** (left), and SSZ-56, **SFS** (right). O atoms have been omitted for better visualization. T atoms in blue denote those that form 4-rings, while orange ones do not.

considered that the degree of B incorporation determined the type of large pore zeolite obtained.[59] We speculated that in the synthesis, B or Al is more easily sited in 4-rings and, therefore, into zeolites with more of such rings. For high silica zeolites with populations of 5- and 6-rings, they are more likely to form with lower T-atom substitution by trivalent ionic centers. Beta zeolite represents a very good example, in contrast to ZSM-12 (**MTW**), which has many of the same subunit features but fewer 4-rings and does not have an Al- or B-rich composition range.

SSZ-82 has 11 unique T atoms in the structure. Eight of the sites are positions which are in 4-rings. The refinement of the structure by Xie et al.[43] had indicated that a better fit was obtained with B in sites T10 and T11. These sites are described as forming the 4-ring sites. These 4-rings separate neighboring 12-rings where there would be accessibility to hydrated Al cations. As pointed out by Xie, the 4-ring sites that could accommodate B, statistically, would be 56/66 (given the multiplicity among the 11 T sites in the unit cell). This would be about 85% of sites.

SSZ-56 by contrast has 14 unique T atoms and 56 in the unit cell. There are 6 of the 14 in 4-ring locations. The population probability now drops to 43%, or about half of what is seen for SSZ-82. It is strongly emphasized in the structural study by Burton and Grosse-Kunstleve[42] that the topology of the 10-rings in SSZ-56 is that of **MEL**. We have shown, once again, in this study that hydrated cations do not access **MEL** domains in SSZ-57. Given the data for the comparison of the zeolites as studied here, one sample of SSZ-82 has almost 50% more B than SSZ-56 in the calcined borosilicate we work with (Table 1a). But Al treatment under constant reaction conditions gives about 120% more Al into SSZ-82 than SSZ-56 (Figure 11). It suggests that there are B tetrahedral sites in SSZ-56 that do not become exchanged for Al. Further, NMR studies are underway to better determine this.

An extension of the 12−10 intersection analysis just given for known structures SSZ-57, -56, and -82 might be a useful guide in solving unknown borosilicate structures in this treatment. With the reactivity, pH leveling near 2, and low efficiency for Al exchange for B sites, SSZ-70 could be considered to fall into this category. Archer et al. had noted, via MASNMR studies, that site connectivity for T atoms in SSZ-70 must be similar in some regards to **MWW**.[49] That would position SSZ-70 to possibly have some exposed 12-ring cups on the exterior. They might thus exchange for Al. But the majority of internal T sites, accessed through 10-rings would exclude Al reinsertion.

In a relevant analysis, B SSZ-70 can be delaminated to UCB-4, having about double the external surface area and, therefore, exposed sites.[46] When the Al reinsertion treatment is carried out on B SSZ-70 and UCB-4, we do see the combined effect of greater pH drop and greater Al uptake for the latter (Table 9). Catalytic studies are underway to take advantage of these enhanced surface sites for large molecule transformations.

Nests versus Defect Sites. We decided to compare the same zeolite structures made as borosilicates and then all-silica, for Al reinsertion capacities. Regarding borosilicate Al reinsertion, we have shown previously, for SSZ-33[38] and here for SSZ-57, that removing B prior to the Al treatment still results in the same degree of lattice substitution as the pH profiles that were virtually identical either during B replacement or if there was no B present (Figure 4). (There is another important outcome of the experiment in comparing pH profiles and Al reinsertion for the host zeolite whether or not the Boron is present. In the case where the boron has not been prehydrolyzed out, there is also some sodium cation (from the synthesis) in these materials. After purposeful acid hydrolysis, of course, they will be removed. What the data tell us is that whether or not the sodium is present has no effect on pH values measured as Al goes back into the host structure nor are we seeing any impeding of hydrolysis rates. In fact, in the data shown in Figure 9, where NMR shows rapid release of boron from SSZ-33, there is some sodium in this borosilicate material, for example.) It is not hard to envision a hydroxyl nest left behind when the B is removed. We actually observed that, in the Al replacement for B in SSZ-33, the hydrolysis of B greatly outpaces the Al uptake. By following the profile, this can be seen, as B increases in solution (NMR results in Figure 9) during the experiment versus the Al content for time points during treatment. Recall that pH drop tracks Al incorporation quite well. Figure 5 gives the pH drop profile for Al into SSZ-33.

There is a small amount of Al measured for the treatment of the all silica zeolite, where we are interested in whether defects can be sites for Al uptake. If we consider that the all-silica zeolite is completely filled by SDA and that it is about 12% of the mass, then we can calculate a "defect" population for the SDA-filled zeolite. The trimethyl adamantyl ammonium cation (C13, H24, N) has a mass of 190. This is roughly 3 times the mass of SiO_2 that contributes 8 times as much to the mass. So our product has a molar ratio of 1 SDA to 24 SiO_2. This would mean that if defect site experienced Al reinsertion, then we would have Si/Al = 24, and the contribution to the product mass would have the Al be more than 10 times what is observed (with a value of Al at 0.15 wt %). So, there is not much evidence for Al reinsertion back into defect sites in the all-SiO_2 zeolite.

The **AFI** structure (one-dimensional, 12-rings) is the second best candidate for the comparison of Al into nests (B AFI), as it has only single OH or O^- sites for anchoring Al (all SiO_2 AFI). Table 11 shows that Al goes into the borosilicate with pH drop to 1.75 and Al content to 0.72 wt %. For the all SiO_2 material there is almost no pH drop. A small amount of Al is observed, but we need to see if it is even tetrahedral.

Open Internal Architecture Impact on Catalysis. As the concepts of shape-selectivity branched out and widened,[1] the size of the pores was no longer the exclusive focus in thinking about shape-selective control in zeolite catalysis. In more recent work an emphasis has been on understanding how confinement (solvent-like) effects in the internal zeolite architecture might impact transition-state behavior in zeolite-catalyzed reactions. Naturally, the spatial details at channel intersections become

dx.doi.org/10.1021/ja4100194 | J. Am. Chem. Soc. 2014, 136, 1462−1471

important[19,23−25] in understanding and predicting product selectivities. It follows that the 12−10 details will be important in such reaction selectivities.

In our recent work on SSZ-57 LP (Al reinsertion) we described the hexane hydroisomerization selectivity to 2,3 and 2,2 (the larger isomer) dimethylbutanes. The SSZ-57 LP shows about a 50% greater production of the smaller isomer at maximum isomer production. The ratio is similar for SSZ-56, another 12−10 system.[21] On the other hand, the pH profile for SSZ-57 and -56 suggests that Al cannot exchange for all sites. The exchange is more thorough for SSZ-82 (12−10) and SSZ-33 (12−12−10). The isomer selectivity for 2,2 dimethylbutane goes up for these latter two zeolites over SSZ-56 and -57. The extent of Al substitution observed and the increase in 2,2 dimethylbutane make both suggest a more open structure at the channel intersection for SSZ-82 and 33. The aqueous acidic Al treatment of borosilicates and the reaction profile (via pH change) thus may be able to predict reaction behavior, related to confinement effect, in future discoveries of novel borosilicate zeolites.

■ CONCLUSIONS

In this study we have explored some of the details of the chemistry of the Al replacement for boron in zeolites. Past work has focused on describing the conditions for complete replacement. Here we look at the pH changes for Al going into the borosilicate lattice starting with dilute aluminum nitrate solutions that have a mildly acidic pH. The pH actually continues to drop as Al is taken up into the lattice, and protons are liberated from the hydrated aluminum +3 cation. Impressive is the fact that the substitution versus pH change is quite linear for a variety of eight zeolites studied. Again we showed that the Al could be reinserted into a nest "vacancy" by first hydrolyzing the boron away form the lattice. Interestingly, the kinetics are about the same for Al going back in whether there is boron there or not. This is not so surprising in that we show that, even under our standard reaction conditions, the boron is leaving faster than the Al goes back in. NMR studies once again show that the Al going back in is found in tetrahedral sites where the boron had been. The new information is that even upon calcination, a majority of the boron in tetrahedral sites is already transformed to trigonal species even before we begin the hydrolysis (again by NMR).

We examined three types of materials. At one boundary extreme is the zeolite **MEL** which has only intersecting 10-rings. We showed, as in earlier studies, that the amount of Al uptake is almost negligible, and almost no protons are generated in the reaction. At the other boundary is the case where all sites can be replaced. This is true of the multidimensional large pore zeolite beta and the SSZ-33, with two large pore systems. Also of interest were the systems where there is some Al replacement but not complete replacement. In this situation we followed Al replacement for boron in known 12−10 ring systems SSZ-56-, 57 and -82 and in unknown SSZ-70. The ability to replace Al for B was variable among them, and insights could be gained from pH profiles. For example, SSZ-56 and -82 both have 12- and 10-ring intersecting pores, but 56 cannot be nearly as well exchanged as 82. A structural comparison that involved looking where B might be in 4-rings, helped to explain those differences. In two cases (SSZ-57 and 70), we also saw that when the initial boron content in the zeolite was higher, a higher final Al (and thus greater pH drop) was achieved. This suggests that the higher B population in a structure has placed a greater number of B tetrahedra in T atom sites where replacement is possible.

We attempted to screen the possibility of Al reinsertion back into lattice defect sites for the zeolites where there had been no B substitution in a synthesis. SSZ-24 (**AFI**) was the large pore one-dimensional system chosen. We can make it with both B substitution and all-silica. After seeing very little uptake in the treatment (and considerable for the B SSZ-24), we concluded that Al does not substitute into defects, unless the zeolite is simply too hydrophobic for this treatment. Borrowing on previous work of Davis and then Koller, we tried the treatment in ethanol (100%) where molecules can be transported into hydrophobic sieves. No Al reinsertion was found under these conditions.

Finally, one of the key benefits from this study raised the issue of how well this treatment might allow one to elucidate the internal pore architecture for unknown borosilicate zeolites. While we initially were attracted to the approach that the extent of pH drop might be the key to the details of pore architecture, it became clear that one had to take the starting boron content into consideration in such an evaluation. We believe that this treatment can impart such useful insight into the details of the host architecture when it is unknown. But the approach that must be taken is to consider the efficacy of boron replacement by Al under a defined set of reaction conditions. For example, under a set of conditions chosen here (which would not allow for complete replacement), the efficacy of Al replacement for B would be 0.50 for SSZ-33, dropping to 0.33 for SSZ-56 and then 0.24 for SSZ-70 when all 3 borosilicates used were in the range of 0.50−0.60 wt % boron in the reactant. Clearly we can see that a material where the boron replacement can be everywhere, such as SSZ-33 or boron beta, gives a higher replacement efficacy under our standard test conditions, where the initial substitution ratio used in the pH study had been Al/B = 0.20. Materials where Al cannot go everywhere are presumably as efficient in the large pore regions as materials like SSZ-33, beta, and SSZ-24, but there is a limit to the access, and that is what we hope to be measuring in terms of an efficacy. We look forward to testing this approach on future novel borosilicate zeolites where the structures may be unknown.

■ ASSOCIATED CONTENT

Ⓢ Supporting Information

Includes graphics of zeolites included in this study and a table of local environment for T atoms in SSZ-82, -33, and -56. This information is available free of charge via the Internet at http://pubs.acs.org.

■ AUTHOR INFORMATION

Corresponding Author

sizo@chevron.com

Notes

The authors declare no competing financial interest.

■ ACKNOWLEDGMENTS

We thank the management of Chevron's Catalyst Department, Charles Wilson, Bob Saxton, and Georgie Scheuerman for support of this research. We thank Dr. Ming Ting Xu (Chevron) for useful discussion on the pH versus Al uptake relationships in our data. We thank Dr. Christopher Lew (Chevron) for the sample of UCB-4. Support of the NMR

facility at Caltech (Beckmann Center) is through NSF grant no. 9724240 and MRSEC Program award no. DMR-520565.

REFERENCES

(1) Degnan, T. F. *J. Catal.* **2003**, *216*, 32−46.
(2) *Database of Zoilite Structures*; IZA-SC: Zürich, Switzerland; http://www.iza-structure.org/databases/.
(3) Zones, S. I. *Microporous Mesoporous Mater.* **2011**, *144*, 1−8.
(4) Kwak, J. H.; Zhu, H.; Lee, J. H.; Peden, C. H. F.; Szanayi, J. *Chem. Commun.* **2012**, *48*, 4758−60.
(5) Kim, J.; Aboulnasr, M.; Lin, L-C; Smit, B. *J. Am. Chem. Soc.* **2013**, *135*, 7545.
(6) Pophale, R.; Daeyaert, F.; Deem, M. W. *J. Mater. Chem. A* **2013**, *1*, 6750−6760.
(7) Chen, C. Y.; Zones, S. I. (ChevronTexaco Corporation). U. S. Patent 6,468,501, 2002.
(8) Lupulesca, A. I.; Rimer, J. D. *Angew. Chem.* **2012**, *51*, 3345.
(9) Mehlhorn, D.; Valuillin, F.; Karge, J.; Cho, K.; Ryoo, R. *Microporous Mesoporous Mater.* **2012**, *164*, 273.
(10) Na, K.; Jo, C.; Kim, J.; Cho, K.; Jung, J.; Seo, Y.; Messinger, R.; Chmelka, B. F.; Ryoo, R. *Science* **2011**, *333*, 328.
(11) de Jong, K. P.; Zecevic, J.; Friedrich, H.; de Jongh, P. E.; Bulut, M.; van Donk, S.; Kenmonge, R.; Finiels, A.; Hulea, V.; Fajula, F. *Angew. Chem., Int. Ed.* **2010**, *49*, 10074.
(12) Serrano, D. P.; Escola, J. M.; Pizzaro, P. *Chem Soc. Rev.* **2013**, *42*, 4004−035.
(13) Haag, W. O.; Lago, R. M; Weisz, P. B. *Faraday Discuss. Chem. Soc.* **1981**, *72*, 317−330.
(14) Chen, N. Y.; Garwood, W. E.; Dwyer, F. G. *Shape selective catalysis in industrial applications*; Marcel Dekker: New York, 1996.
(15) Csicsery, S. M. In *Catalysis by Microporous Materials, Studies in Surface Science and Catalysis*; Beyer, H. K., Nagy, J. B., Karge, H. G., Kinsii, I., Eds.; Elsevier: Amsterdam, 1995.
(16) Santilli, D. S. *J. Catal.* **1986**, *99*, 327.
(17) Garces, J. M.; Olken, M. M.; Lee, G. J.; Meima, G. R.; Jacobs, P.; Martens, J. *Top. Catal.* **2009**, *52*, 1175−81.
(18) Adair, B.; Chen, C. Y.; Wan, K. T.; Davis, M. E. *Microporous Mater.* **1996**, *7*, 261.
(19) (a) Frillete, V. J.; Haag, W. O.; Lago, R. M. *J. Catal.* **1981**, *67*, 218. (b) Zones, S. I.; Harris, T. V. *Micro. Meso. Mat.* **2000**, 31−46. (c) Carpenter, J.; Yeh, S. W.; Zones, S. I.; Davis, M. E. *J. Catal.* **2010**, *269*, 64−70.
(20) Haag, W. O. In *Zeolites and Related Microporous Materials: State of the Art*; Weitkamp, J., Holderich, W., Eds.; Elsevier: Amsterdam, 1994.
(21) Chen, C. Y.; Ouyang, X.; Zones, S. I.; Banach, S. A.; Elomari, S. A.; Davis, T. M.; Ojo, A. F. *Microporous Mesoporous Mater.* **2013**, *169*, 248.
(22) Olsbye, U.; Bjorgen, M.; Svelle, S.; Lillerud, K-P; Kolboe, S. *Catal. Today* **2005**, *106*, 108−11.
(23) Davis, T. M.; Chen, C. Y.; Ojo, A. F.; Zilkova, N.; Vitrarova-Prochazkova, D.; Cejka, J.; Zones, S. I. *J. Catal.* **2013**, *298*, 84−93.
(24) Gounder, R.; Iglesia, E. *Ang. Chem. Int. Ed.* **2010**, *49*, 808−811.
(25) Bhan, A.; Iglesia, E. *Acc. Chem. Res.* **2008**, *41*, 559.
(26) Matias, P.; Lopes, J. M.; LaForge, S.; Magnoux, P.; Guisnet, M.; Ribeiro, F. R. *Appl. Catal., A* **2008**, *351*, 174−183.
(27) Gounder, R.; Iglesia, E. *Chem. Commun.* **2013**, *49*, 3491−3501.
(28) Gounder, R.; Iglesia, E. *Angew. Chem., Int. Ed.* **2010**, *49*, 808−811.
(29) Sastre, G.; Corma, A. *J. Mol. Catal. A.* **2009**, *305*, 3−7.
(30) Carr, R. T.; Iglesia, E.; Neurock, M. *J. Catal.* **2011**, *278*, 78−93.
(31) Burton, A. W.; Zones, S. I.; Elomari, S.; Chan, I. Y.; Chen, C. Y.; Hwang, S-J; Ong, K. *Stud. Surf. Sci. Catal.* **2007**, *170A*, 690−697.
(32) Zones, S. I.; Ruan, J.; Elomari, S.; Terasaki, O.; Chen, C. Y.; Corma, A. *Solid State Sci.* **2011**, *13*, 706−713.
(33) Ruan, J. Ph.D. Thesis, Stockholm University, Stockholm, Sweden, 2008.
(34) Baerlocher, C.; Weber, T.; McCusker, L. B.; Palatinus, L.; Zones, S. I. *Science* **2011**, *333*, 1134−7.
(35) Zones, S. I.; Chen, C. Y.; Corma, A.; Cheng, M. T.; Kibby, C. L.; Chan, I. Y.; Burton, A. W. *J. Catal.* **2007**, *250* (1), 41−54.
(36) Degnan, T. F. *J. Catal.* **2003**, *216*, 32−46.
(37) Chen, C. Y.; Zones, S. I.; Huang, S-J; Bull, L. M. *Stud. Surf. Sci. Catal.* **2004**, *154(B)*, 1547−1554.
(38) Chen, C. Y.; Zones, S. I. In *Zeolites: Synthesis, Catalysis and Applications*; Cejka, J., Corma, A., Zones, S. I., Eds.; Wiley Interscience: Hoboken, NJ, 2011, pp156−170.
(39) Zones, S. I.; Chen, C. Y.; Benin, A.; Hwang, S.-J. *J. Catal.* **2013**, *308*, 213−225.
(40) Zones, S. I. U.S. Patent 4,963,337, 1990.
(41) Zones, S. I.; Burton, A. W. U.S. Patent 7,108,843, 2006.
(42) Elomari, S.; Burton, A.; Medrud, R. C.; Grosse-Kunstleve, R. *Microporous Mesoporous Mater.* **2009**, *118*, 325−33.
(43) (a) Xie, D.; Mccusker, L.; Baerlocher, C. *J. Am. Chem. Soc.* **2011**, *133*, 20604−610. (b) Burton A. W., EP 2370360A2, 2011.
(44) Holtermann, D. L.; Jossens, L. W.; Rainis, A.; Santilli, D. S.; Ziemer, J. N.; Zones, S. I., U.S. Patent 5,693,215, 1997.
(45) Zones, S. I.; Nakagawa, Y. *Microporous Mater.* **1994**, *2*, 557−62.
(46) Ogino, I.; Zones, S. I.; Xie, D.; Ouyang, X.; Katz, A. S. *Chem. Mater.* **2013**, *25* (9), 1502−1509.
(47) Nakagawa, Y., U.S. Patent 5,645,812, 1997.
(48) Ogino, I.; Zones, S. I.; Katz, A. General Heteroatom-Tolerant Method for Delaminaiton of Layered Zeolite Precursors. Proceedings of the ZMPC 2012 International Symposium on Zeolites and Microporous Crystals, Hiroshima, Japan, July 28-August 1, 2012.
(49) Archer, R.; Carpenter, J. R.; Hwang, S.-J.; Burton, A. W.; Chen, C. Y.; Zones, S. I.; Davis, M. E. *Chem. Mater.* **2010**, *22*, 2563−2572.
(50) Stromaier, K. In *Zeolites and Catalysis*; Corma, A., Cejka, J., Zones, S. I., Eds.; Wiley-VCH: Weinheim, Germany, 2010, Chapter 2.
(51) Shantz, D. F; auf der Gunne, J. S.; Lobo, R. F.; Koller, H. *J. Am. Chem. Soc.* **2000**, *122*, 6659.
(52) Roman-Leshkov, Y.; Davis, M. E. *ACS Catalysis* **2011**, *1*, 1566−1580.
(53) Huong, T. T.; Koller, H. *Microporous Mesoporous Mater.* **2012**, *148*, 80−87.
(54) Hwang, S-J; Chen, C. Y.; Zones, S. I. *J. Phys. Chem. C* **2004**, *108*, 18535−546.
(55) Baes, C. F.; Mesmer, R. E. *Hydrolysis of Cations*; Wiley: New York, 1976.
(56) Gil, B.; Zones, S. I.; Hwang, S-J; Bejblova, M.; Cejka, J. *J. Phys. Chem C* **2008**, *112*, 2997−3007.
(57) Corma, A. *Microporous Mesoporous Mater.* **1998**, *21*, 487.
(58) Simancas, R.; Dari, D.; Velamazan, N.; Navarro, M. T.; Cantin, A.; Jorda, J. L.; Sastre, G.; Corma, A.; Rey, F. *Science* **2010**, *330*, 1219.
(59) Zones, S. I.; Nakagawa, Y.; Harris, T. V.; Yuen, L-T *J. Am. Chem.* **1996**, *118*, 7558−7567.